The Galactic Cosmic Ray Simulator at the NASA Space Radiation Research Laboratory

Lisa C. Simonsen,[1] Tony C. Slaba, [1] Peter Guida,[2] and Adam Rusek[2]

[1] NASA Langley Research Center, Hampton, Virginia USA
[2] Brookhaven National Laboratory, Brookhaven, New York USA

Correspondence email: lisa.c.simonsen@nasa.gov

I. ABSTRACT

With NASA's new Artemis plan for a sustainable return to the moon, astronauts will once again leave Earth's protective magnetosphere only to endure higher levels of radiation from galactic cosmic radiation (GCR). The ever penetrating GCR will continue to pose significant health risks especially as lunar missions increase in duration and as NASA sets its aspirations on Mars. The primary risks of concern include carcinogenesis, central nervous system (CNS) effects resulting in potential in-mission cognitive or behavioral impairment and/or late neurological disorders, and degenerative tissue effects including circulatory and heart disease. Characterization and mitigation of these risks requires a significant reduction in the large biological uncertainties of chronic (low-dose rate) heavy ion exposures and the validation of countermeasures in a relevant space environment. Historically, most research on understanding space radiation-induced health risks has been performed using acute exposures of monoenergetic single-ion beams. However, the space radiation environment consists of a wide variety of ion species over a broad energy range. Using the fast beam switching and controls systems technology recently developed at the NASA Space Radiation Laboratory at Brookhaven National Laboratory, a new era in radiobiological research is possible. NASA has developed the "GCR simulator" to generate a spectrum of ion beams that approximates the primary and secondary GCR field experienced at human organ locations within a deep-space vehicle.

II. INTRODUCTION

The goal of NASA's space radiation research program is to enable the human exploration of space beyond low-Earth-orbit (LEO) with acceptable risk and mitigation strategies in place to ensure the health, safety, and productivity of our crew. With quick-paced Artemis Moon-to-Mars program goals, NASA is committed to landing American astronauts on the Moon by 2024 and establishing sustainable lunar missions by 2028 in preparation for sending astronauts to Mars [1]. The mitigation of health risks from both intermittent solar particle events (SPEs) and chronic galactic cosmic radiation (GCR) will become more challenging as crew leave the protection provided by the Earth's magnetosphere. Although improved storm shelter designs, space weather forecasting, and operational dosimetry can significantly reduce the risk of acute radiation syndromes from a large SPE, the potential for in-mission health and performance decrements as well as the risk of long-term health consequences from chronic exposure to GCR remain a significant challenge to characterize and mitigate for long duration missions [2,3]. Physical shielding strategies designed to significantly reduce the health risks from GCR become prohibitively costly because of the high charge (Z) and energy (E) of the primary constituent particles, referred to as high charge and high energy (HZE) particles, and from the production of secondary protons, neutrons, and heavier fragments produced as a result of interactions with spacecraft shielding and human tissues [4]. These heavy ions, low energy protons, and helium ions are highly ionizing forms of radiation with spatial distributions of radiation deposition, or energy loss, in tissue that are very different from those caused by common forms of radiation found on Earth, namely x-rays and gamma rays [5]. The biological effects of these ions are poorly understood.

Characterizing the biological response of cells, tissues, and animal models in a relevant space environment and understanding the qualitative differences in biological damage compared with terrestrial radiation is essential in establishing and/or validating models of risk, establishing permissible exposure limits (PELs), and developing effective countermeasure strategies to enable safe, long-duration space travel. In 2003, NASA commissioned the NASA Space Radiation Laboratory (NSRL) at Brookhaven National Laboratory (BNL) with a dedicated beamline

and laboratory space to conduct ground-based, heavy-ion research [6]. The facility is capable of supplying particles from protons to gold. Available beam energies range from 50-2500 MeV for protons and 50-1500 MeV/n for ions between helium and iron. Heavier ions from charge Z = 27-79 are limited to ~350-500 MeV/n [https://www.bnl.gov/nsrl/]. Over the last decade, facility investments in ion-source and controls technology enabled the fast switching of ion-energy beam combinations from an automated list of hardware settings in a predetermined sequential order to more closely approximate exposures in space. With input from an international community of physicists and radiobiologists [7], NASA has developed a "GCR simulator" at BNL for principal-investigator (PI) led research studies. This new capability is currently being used to inform our understanding of space radiation effects on the risk of cancer, central nervous system decrements, and cardiovascular disease endpoints and to establish a ground-based, space-relevant environment to test countermeasure efficacy.

III. METHODS AND MODELS

Three key areas were considered in concert to design the GCR simulator including: 1) defining mission relevant radiation environments and resulting exposures; 2) accounting for NSRL facility limitations and completing required hardware and software upgrades; and 3) accounting for constraints imposed by the care and handling of animals and cellular studies as shown in Fig 1. The design of the irradiation field must consider aspects important to each of the major health risk areas. For example, a simpler particle field may be adequate to characterize cancer compared with a more complex field that may, or may not, be required to characterize CNS decrements. The validation of countermeasures in what is defined as a "space relevant environment" may require additional complexities in field description.

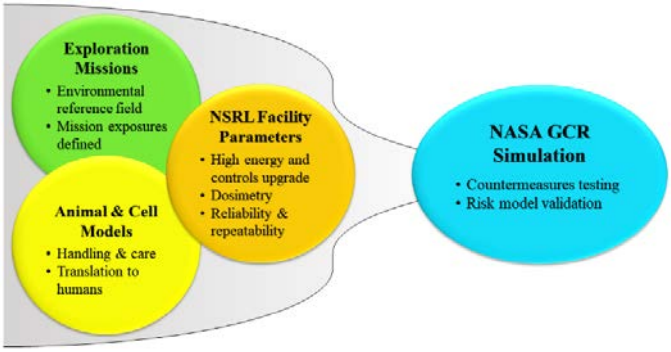

Fig 1. Three key areas that must be developed together to ultimately provide the GCR simulator at NSRL. Development focused on establishing irradiation requirements and balancing facility capabilities and limitations including constraints imposed by animal and cellular model systems.

III.I Development Approach

III.I.I Galactic Cosmic Ray Environment

Galactic cosmic rays originate outside the solar system and are likely formed by explosive events such as supernova. They consist of the nuclei of the chemical elements, from hydrogen to uranium, which have been accelerated to extremely high energies outside our solar system. The energy spectra of all GCR particles are very broad with the region extending from ~10 MeV/n to 50 GeV/n being of primary importance to space applications [4,8,9]. Within our solar system, the solar wind modulates the flux of galactic cosmic rays over an approximate 11 year cycle with an intensity that is inversely correlated with solar activity. During phases of higher solar activity, the GCR intensity is at a minimum while at solar minimum, the GCR intensity is maximal. At solar maximum, the cosmic-ray flux is decreased by a factor of 3 to 4 compared to solar minimum [4], while exposure estimates behind typical spacecraft shielding are reduced by roughly a factor of two [10,11].

The free space GCR environment (Fig 2A) is modified as it passes through spacecraft materials as a result of atomic and nuclear interactions producing an internal environment comprised of both primary and secondary radiation including energetic neutrons, protons, helium ions, and other nuclear fragments ($Z \geq 3$). While heavy ion contributions to dose and dose equivalent in free-space and behind light shields (on the order of 5 g/cm^2) are large [4], behind typical spacecraft shielding dose and dose equivalent are dominated by protons and light ions [12,13]. Further attenuating the radiation field is an astronaut's body self-shielding. Average spacecraft shielding is on the order of 10 to 20 g/cm^2 [12] while the human body has an average tissue thickness of ~30 g/cm^2 for internal organ locations [14]. The modulation of the free space environment at these combined thicknesses can be seen in Fig 2B. The GCR simulator is designed to approximate this mixed field of primary and secondary particles seen at critical body organ and tissue locations within an astronaut in a shielded vehicle. In comparison with the high energies of GCR in the 10's of GeV/n, NSRL's upper energy limit of 1.5 to 2.5 GeV/n will be the largest constraint on implementation strategy.

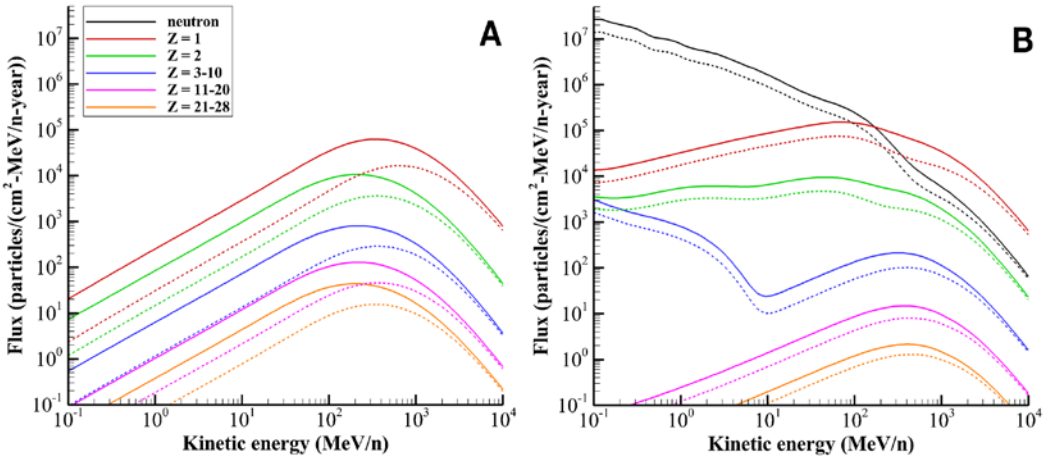

Fig 2. GCR particle spectra at solar minimum conditions (June 1976) denoted by solid lines and solar maximum conditions (June 2001) denoted by dashed lines in (A) free space and (B) behind 20 g/cm^2 of aluminium to female blood forming organs (BFO) as described by the Badhwar-O'Neill 2010 GCR model [15], HZETRN transport code [16,17,18], and human phantoms [14,19,20].

III.I.II Mission Doses

Over the last decades, there have been numerous studies estimating radiation exposures to astronauts from both solar particle events and galactic cosmic radiation during solar minimum and maximum conditions. These studies have assumed a wide variety of vehicle and shielding configurations with various levels of fidelity in design and material characterization, mission durations, and solar conditions [21,22,23]. Over the years, environmental models, transport codes, nuclear models, and human voxel phantoms have greatly improved our ability to more accurately project exposures [24]. Additionally, important environmental measures by NASA's Mars Science Laboratory's Radiation Assessment Detector (MSL-RAD) have provided important benchmark data to understand where models may have sometimes underestimated projected exposures [25,26]. The following estimates of mission exposures have been compiled to guide radiobiology experiments at NSRL and are largely representative of solar minimum conditions (when GCR flux is at its maximum). Mission exposure estimates include primary and secondary radiation generated in shielding and tissue with neutrons contributing roughly 1% of the dose (10% dose equivalent) in free space vehicles, <5% of dose (20% dose equivalent) within lunar surface habitats [27], and <5% of dose (25-30 % dose equivalent) on Mars surface [28]. The range of values is representative of numerous assumptions and caveats of the individual historically-based study details, as well as, efforts to maintain direct comparison with environmental measurements [29].

Table 1: Summary of Exploration Mission Exposures beyond low Earth orbit.

	Mission Duration	Dose (mGy)	Gray Equivalent (mGy-Eq)[a]	Dose Equivalent (mSv)[b]
Sortie to Gateway (free-space)	30 days	20	35	55
Lunar Surface Mission (2 weeks on surface)	42 days	25	45	70
Sustained Lunar Operations	1 year	100 - 120	180 - 220	300 – 400
Deep-Space Habitat	1 year	175 - 220	300 - 400	500 - 650
Mars Mission	650 to 920 days	300 - 450	550 - 800	870 - 1200

[a]Conversion of dose to gray equivalent uses RBE values recommended by NCRP No. 132 [30]
[b]Both NASA defined quality factors [31] and ICRP 60 quality factors [32] considered in range of estimates.

Considering the mission exposures in Table 1, relevant GCR doses are 125, 250, 500, and 750 mGy for radiobiology experiments at the NSRL. These doses span the exploration missions under consideration by NASA used for assessing risk posture and the need for countermeasure development. A higher exposure of 750 mGy is included to establish a dose response curve above expected mission exposures supporting the evaluation of mixed-field quality effects to inform permissible exposure limits. In some cases where clinically significant endpoints are difficult to discern in animal model systems at lower doses, such as the determination of quality effects on the cardiovascular system, exposures up to 1.5 Gy may be warranted.

III.I.III Comparison of Implementation Strategies

The simulator is designed to expose animal models and cell culture systems to the environment seen by crew at critical body organ and tissue locations within shielded vehicles - where the external GCR environment is transported through the vehicle shield geometry and then through the self-shielding provided by the body. Three basic implementation strategies were considered (Fig 3): an external field approach, a local tissue field approach, and a hybrid approach. A) In the external field approach, discrete NSRL beams are selected to represent the free-space, external GCR field, and the biological target is placed behind shielding materials in the beam line. The shielding material is sized to modify the primary beams in a manner similar to spacecraft and body-self (tissue) shielding. B) In the local tissue field approach, models are used to characterize the spectrum of particles and energies occurring in critical body organs behind shielding. This modified spectrum is then represented in the accelerator with discrete monoenergetic beams that are delivered directly to the biological target with no intervening shield material in the beamline. C) The hybrid approach considers a lesser amount of shielding within the beamline with variable tissue equivalent material thicknesses. The goal of this approach is to generate secondary particles with a spread in energy and charge and to allow for correlated secondary ion interactions within cells. The tissue equivalent shielding also provides a moderator that may be scaled to account for the different physical sizes of animal models. In this case, the external field (of higher energies than local tissue approach) and simulated vehicle and tissue shielding (less shielding than used with the external field approach) would be modified to best represent the particle spectrum seen within an astronaut.

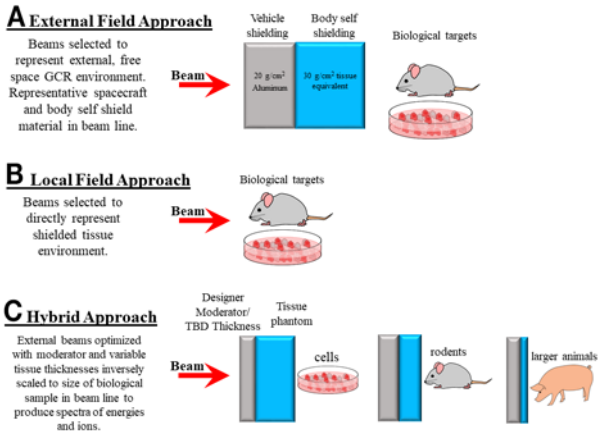

Fig 3. Three basic strategies for beam selection. (A) Beam selection is representative of the external, free-space GCR spectrum and is approximated by discrete ion and energy beams delivered onto a shielding and tissue equivalent material placed within the beam line, in front of the biological target. (B) Beam selection is representative of the shielded tissue spectrum found in space (e.g., average tissue flux behind vehicle shielding) and is approximated by discrete ion and energy beams delivered directly onto the biological target. (C) Beam selection is representative of energies less than free space with thinner amounts of vehicle shielding and variable thicknesses of tissue equivalent materials to represent the differences in body self-shielding between the physical sizes of species.

The first two approaches were thoroughly analyzed by Slaba and colleagues, 2016 [11] considering simple shield geometries of 5, 10, and 20 g/cm^2. Analysis showed that the NSRL upper energy constraints limit the feasibility of simulating the external, free space GCR spectrum directly. In particular, it was shown that approximately half of the exposure behind shielding is lost if the energies above ~1.5 GeV/n cannot be represented in the external field. However, the shielded, local tissue environment can be reasonably well represented, with approximately 85% of effective dose captured, within current facility capabilities with energies of protons up to 2.5 GeV, helium up to 1.5 GeV/n, and heavier ions up to 1.5 GeV/n. To achieve this same effectiveness for the external field approach, upper energy limits would need to be increased to approximately 5 GeV/n to 8 GeV/n depending on estimated shield thicknesses used in the beamline. Thus, the GCR simulator is designed to approximate a reference environment based on the local tissue approach to best describe mission exposures encountered by the crew (Fig 3B). While a very limited number of neutrons are produced from interactions with exposure boxes, culture dishes, and tissues, relatively few neutrons (or pions/muons for that matter) compared with mission exposures interact directly with the biological target. However, the dose from recoil protons can and is accounted for in the local field approach (See Section III.II) Future work, including neutron generation, will consider the advantages and disadvantages of a hybrid approach.

III.II Determination of GCR Reference Environment

Radiation exposure to the crew is mission specific and dependent on multiple factors such as mission destination and duration, vehicle design, and solar conditions. Through the analysis of Slaba and colleagues, 2016 [11], the GCR reference field was chosen as the female BFO spectrum behind 20 g/cm^2 of aluminum shielding during solar minimum conditions. It was found that variation in dose, dose equivalent, and LET spectrum introduced by shielding geometry and identification of the BFO to represent critical organ and tissue exposures is likely small compared with uncertainties associated with facility limitations in representing the full reference field by a discrete number of monoenergetic beams. The tissue energy and LET spectra behind shielding and calculated dose per particle type was used to guide NSRL beam delivery requirements.

Characteristics of the reference field are shown in Fig 2 comparing the free-space GCR ion spectral flux as a function of energy to the attenuated spectrum within tissue. The build-up of secondary protons, light ions, and neutrons can be seen compared to the attenuation of heavy ions. In the BFO behind 20 g/cm^2, the Z = 1 ions account for ~64% of dose, the Z = 2 ions account for ~17% of dose, and ions of $Z \geq 3$ contribute ~7% of dose as shown in Table 2. The analysis of Slaba and colleagues, 2016 [11] showed that the HZE particles with the largest contribution

to dose in the reference field were: C, N, O, Ne, Mg, Si, Ca, and Fe which make-up 69% of the HZE dose. This is not surprising considering the relative abundance of HZE particles in the natural GCR spectrum.

It is important to clarify how the contributions of secondary neutrons to dose, through elastic and inelastic collisions occurring within tissue, are evaluated. The radiation transport code, HZETRN [16,17,18] used to calculate reference field quantities, propagates secondary neutrons and any of their reaction products with charge of $Z \leq 2$. Of particular interest are the recoil protons generated within tissue by mainly low energy neutrons. These protons are explicitly included in the Z=1 component of the reference environment and are well represented in the GCR simulator by the binary filter approach (See Beam Selection Section) implemented for protons with energy < 100 MeV. Heavy target fragments ($Z \geq 3$) produced from inelastic neutron interactions, with approximately 0.8% dose contribution, are not explicitly included in the reference environment. These neutron interaction products will contribute more significantly (~10%) to biologically weighted exposure quantities such as dose equivalent or risk of exposure induced death (REID). In the local field approach, these particles are not directly simulated in the NSRL beam line. Likewise, π/EM cascades, which contribute approximately 11% to dose, are also not explicitly represented in the GCR simulator. Contributions to dose are normalized in Table 2 excluding the contribution of these two component of the spectrum. Thus, the GCR simulator beam selection is designed to deliver the majority of the dose from hydrogen (~65-75%) and helium ions (~10-20%) with heavier ions ($Z \geq 3$) contributing the remainder (6-8%).

Table 2. Average tracks per cell nucleus per year, dose D (mGy/year), and percent contribution of particles to dose for reference field during 1 year solar minimum and normalized to 500 mGy.

Particle type	**Average tracks per cell nuclei[a]**	**Dose (mGy/Year)**	**Percent contribution (%)**	**Dose distribution normalized to 500 mGy**	**Percent contribution of normalized dose to 500 mGy (%)**
π/EM	0.1	15.5	11.6	0	
Neutron	N/A	1.1[b]	0.8	0	
hydrogen	126	86[c]	64.2	366.3	73.3
helium	7	22.5[d]	16.8	95.8	19.2
HZE	0.5	8.9	6.6	37.9	7.6
total	133.6	134	100	500	100

[a]Assumes a cell nucleus cross section of 100 μm^2
[b]Dose exclusively from heavy target fragments ($Z \geq 3$) produced from inelastic neutron interactions.
[c]Includes contributions from elastic and inelastic reaction products of Z=1 from neutron interactions.
[d]Includes contributions from inelastic reaction products of Z=2 from neutron interactions.

The reference field spectral quantities and integral quantities provide a means to optimize the selection of beam parameters. The neutron, hydrogen, and helium energy spectra from the reference field are shown in Fig 4A. The hydrogen spectrum includes protons (^{1}H), deuterons (^{2}H), and tritons, (^{3}H), and the helium spectrum includes helions (^{3}He) and alphas (^{4}He). These spectra explicitly include elastic and inelastic reactions products from neutron interactions. Panel B shows the total differential LET spectrum of the reference field and the differential LET spectrum without the hydrogen and helium contributions. The quantity plotted on the vertical axis, fluence, has also been scaled by LET to improve plot clarity. Integrating under the curves shown in Fig 4 yields the total annual dose (standard constants to convert from MeV/g to Gy would need to be applied) of 134 mGy (shown in Table 2**).** The tissue energy spectra of protons and helium particles and the tissue LET spectrum of heavier charged particles of ($Z \geq 3$) behind shielding are used to guide the selection of NSRL beams.

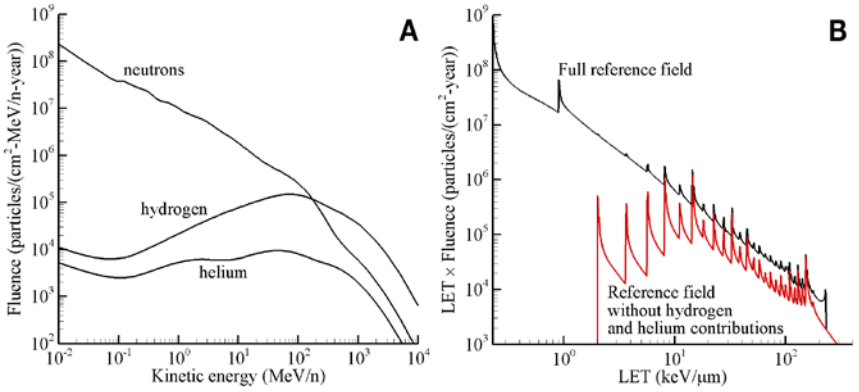

Fig 4. Reference field spectra in the female BFOs behind 20 g/cm^2 of aluminum shielding during solar minimum conditions. (A) Neutron, hydrogen, and helium energy spectra. (B) The corresponding differential LET spectra with and without contributions from hydrogen and helium. Based on calculations from Slaba [11].

III.III Implementing the GCR Simulator at the NSRL

In early 2017, the GCR simulator reference field (Fig 4) was baselined by NASA for implementation at the NSRL. A single reference field was defined to ease requirements on facility operations, to enhance cross comparison of radiobiological results between principal investigator teams, and to increase return on investment for secondary science objectives through tissue sharing. Although the primary and secondary field of GCR is comprised of a spectrum of many ions over a broad energy range, early simulation at NSRL was limited to relatively few monoenergetic beams to maintain reliability and repeatability.

III.III.I Beam Selection

Several key decisions were made in efforts to define and demonstrate an early baseline capability to accelerate NASA research objectives. First, the reference spectrum was defined in terms of the physical quantities of flux versus energy and flux versus LET as described in the previous section. The Z = 1, Z = 2, and Z $\geq$ 3 portions of the reference field were considered individually. Beam selection favored those ions with a wealth of historical radiobiological data, ions that provided LET and energy coverage of the reference field as well as consideration of their contribution to biological damage relative to the International Commission on Radiological Protection (ICRP) quality factor weighting [30]. In addition to beam energy, the number of discrete monoenergetic ions was thought to be limited by the production capability within the Electron Beam Ionization Source (EBIS) to six to eight ions with no more than two gases being used as sources. The general scheme is notionally illustrated in Fig 5.

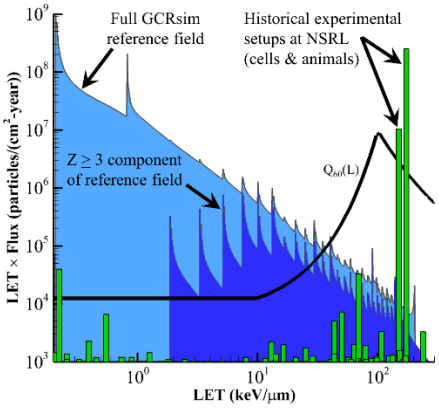

Fig 5. Illustration of beam selection strategy for GCR simulator. The total LET spectrum (light blue) and the HZE spectrum (dark blue) are shown separately. The green bars are representative of the number of single ion beam

experiments performed at NSRL as a function of LET (scaled for plot clarity). The black line is representative of ICRP-60 quality factor weighting [32] to estimate biological damage (scaled for plot clarity).

From an historical perspective at NSRL, the most used ions (as represented by the green bars on Fig 5) include iron (1000 MeV/n, 600 MeV/n), protons (1000 MeV/n, 150 MeV/n), silicon (600 MeV/n, 300 MeV/n), with fewer runs of titanium (1000 MeV/n), oxygen (600 MeV/n, 250 MeV/n), and carbon (290 MeV). Given that hydrogen and helium account for a large fraction of overall fluence and dose over a broad energy range, these particle are given the greatest emphasis in beam selection and are handled individually. Monoenergetic particles are selected to represent the physical quantity of flux over a specific energy (MeV) range. This separates the contributions of protons from helium in regions where LET values overlap. The NSRL's binary filter will be used to generate a "continuous" low energy spectrum of proton and helium particles below 100 MeV/n. The binary filter is a variable thickness degrader system made of polyethylene (density of 0.93 g/cm^3) sheets that can be remotely inserted into the beamline to slow down or stop incoming particles (See NSRL Facility Modifications Section). Although NSRL can generate lower energy protons and alphas down to 50 MeV/n, utilizing the binary filter allows for more efficient operations, requiring a fewer number of discrete beam energies (less energy switching) and provides a reasonably smooth dose distribution (similar to approximating a spread-out Bragg peak) within the biological target. A smaller number of specific monoenergetic HZE beams are selected to collectively represent the associated HZE or high-LET portion of the reference spectrum in which multiple ions may contribute within a range of LET values. The implementation of this strategy is shown in Fig 6.

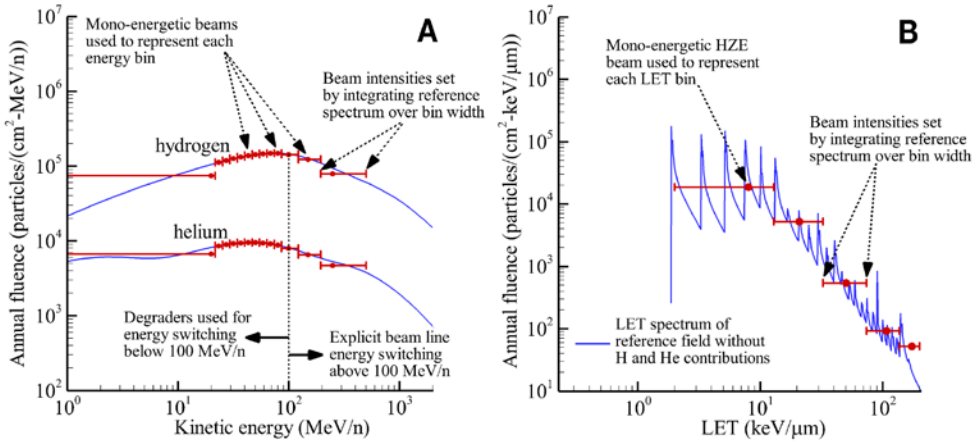

Fig 6. Representation of the reference field using discrete monoenergetic beams. The hydrogen and helium energy spectra are considered directly (A), whereas HZE ions are represented within the LET spectrum (B). Solid blue lines are the reference spectra from Fig 6. The bin widths for 1GeV/n protons and helium particles are at lower fluences and not shown on the figure, however these data are included in supplementary data file.

Selection of discrete proton and alpha beams included 1000 MeV/n and 250 MeV/n based on historical data and the additional beams of 150 MeV/n and 100 MeV/n to capture energy range of interest. It was decided to use mon-energetic beams of protons and alphas of the same energies (MeV/n). To establish the proton and alpha intensities to be delivered by the beam, discrete energy bins were assigned to each of the monoenergetic ions with the corresponding intensity determined by integrating the reference field over the indicated energy bin to obtain total fluences. Below 100 MeV/n, discrete proton and alpha beam energies are achieved by using the polyethylene degrader system. Ten log-spaced energy bins were defined between 20 MeV/n and 100 MeV/n. It was recognized that protons and alphas below 20 MeV/n would not have sufficient energy to penetrate through the animal exposure boxes (~2 mm of polyethylene) and reach radiosensitive organs. Therefore, 20 MeV/n was the lowest beam energy used and the lower bin limit was set to 0 MeV/n for integration to capture the total fluence of protons and alphas contributing to reference field integral quantities. As will be seen, the entrance dose of the 20 MeV/n beams may appear artificially high compared with the next highest energy, but will contribute negligibly to internal exposures and biological outcomes. Above 100 MeV/n, proton and alpha beams are delivered directly by the accelerator at the four selected energies. The proton and alpha energy bin limits above 100 MeV/n are determined by considering the geometric mean of adjacent

energies. To establish the upper bin width for integration represented by the 1 GeV/n beams, the upper energy limit was set at 50 GeV/n for both protons and alphas.

For ions of $Z \geq 3$, the LET domain is separated into five discrete, log-spaced bins as shown in Fig 6B. Based on historical data and requirement to cover the range of LET values represented by ions with $Z \geq 3$, the following HZE beams were selected for the reference field: ^{12}C (1000 MeV/n) and ^{16}O (350 MeV/n) were selected to be representative of particles of $3 \leq Z \leq 9$; and ^{28}Si (600 MeV/n), ^{48}Ti (1000 MeV/n), and ^{56}Fe (600 MeV/n) were selected to be representative of particles of $Z \geq 10$. To set the HZE beam intensities, discrete LET bins were assigned to each of the five monoenergetic ions with the corresponding intensity determined by integrating the reference field over the indicated LET bin to obtain total fluences. For carbon, the lower bin limit is set to 2 keV/μm which corresponds to the lowest LET for Z = 3 ions in water. The upper bin limit is set as the geometric mean of the carbon and the adjacent oxygen LET value (found to be 12.9 keV/μm). Bin limits for oxygen, silicon and titanium are similarly defined by considering the geometric mean of LET values for adjacent beams. For iron, the upper LET bin limit was selected as 200 keV/μm to capture the region important to biological systems beyond which RBE continues to decrease as $\sim 1/LET^{0.5}$.

Following the beam selection strategy discussed above, the reference field is specifically defined by the ion-energy beam combinations shown in Table 3. The sequentially delivered mixed field consists of 33 beams including 4 proton energies plus degrader, 4 helium energies plus degrader, and the five heavy ions of ^{12}C (1000 MeV/n), ^{16}O (350 MeV/n), ^{28}Si (600 MeV/n), ^{48}Ti (1000 MeV/n), and ^{56}Fe (600 MeV/n). A binary polyethylene filter is used with the 100 MeV/n H and He beams to provide the distribution of low-energy particles between 80 and 20 MeV/n. The NSRL GCR simulator reference field is normalized to a Mars mission relevant exposure of 500 mGy as shown in Table 3. Other doses of interest are 125, 250, and 750 mGy depending on animal model, endpoints, and animal numbers required for statistical significance. These doses are implemented as fractions or multiples of Table 3.

Table 3. "NSRL GCR Simulation" beam definition normalized to 500 mGy.

Primary ion-energy beam combinations in GCR Simulator

Ion	E (MeV/n)	LET (keV/ μm)	Range (cm)	Dose (mGy)	Fractionated dose- 24 exposures (mGy/day)
^{1}H	20 - 100	*Polyethylene degrader to lower energies*		140.6	5.86
^{1}H	150	0.54	15.9	35	1.46
^{1}H	250	0.39	38.1	68.9	2.87
^{1}H	1000	0.22	326.6	123.6	5.15
^{4}He	20 - 100	*Polyethylene degrader to lower energies*		39.6	1.65
^{4}He	150	2.17	16	7.5	0.31
^{4}He	250	1.56	38.3	16.4	0.68
^{4}He	1000	0.88	327.8	24.9	1.04
^{12}C	1000	7.95	110.13	11.7	0.49
^{16}O	350	20.8	16.95	15.4	0.64
^{28}Si	600	50.2	22.73	8.1	0.34
^{48}Ti	1000	109.5	32.53	4.5	0.19
^{56}Fe	600	175.1	13.09	4.1	0.17
			Total	*500*	*20.8*

Ten lower energy proton beams from 100 MeV/n proton incident on degrader system

Ion	E (MeV/n)	LET (keV/ µm)	Range (cm)	Dose (mGy)	Fractionated dose- 24 exposures (mGy/day)
^{1}H	20	2.59	0.43	30.4	1.3
^{1}H	23.3	2.29	0.56	6.7	0.3
^{1}H	27.2	2.02	0.75	7.4	0.3
^{1}H	31.7	1.79	0.98	8	0.3
^{1}H	37	1.58	1.3	8.7	0.4
^{1}H	43.2	1.39	1.72	9.3	0.4
^{1}H	50.3	1.23	2.26	10	0.4
^{1}H	58.7	1.09	2.99	10.6	0.4
^{1}H	68.5	0.97	3.95	11.1	0.5
^{1}H	79.9	0.86	5.2	11.2	0.5
^{1}H	100	0.73	7.76	27.2	1.1

Ten lower energy helium beams from 100 MeV/n helium particle incident on degrader system

Ion	E (MeV/n)	LET (keV/ µm)	Range (cm)	Dose (mGy)	Fractionated dose- 24 exposures (mGy/day)
^{4}He	20	10.34	0.43	11	0.5
^{4}He	23.3	9.14	0.57	2.1	0.1
^{4}He	27.2	8.06	0.75	2.2	0.1
^{4}He	31.7	7.12	0.99	2.3	0.1
^{4}He	37	6.29	1.31	2.5	0.1
^{4}He	43.2	5.56	1.73	2.6	0.1
^{4}He	50.3	4.92	2.28	2.7	0.1
^{4}He	58.7	4.36	3.01	2.7	0.1
^{4}He	68.5	3.86	3.97	2.7	0.1
^{4}He	79.9	3.43	5.23	2.7	0.1
^{4}He	100	2.9	7.81	6.1	0.3

A number of radiobiology studies have indicated that the order of exposure to protons and heavy ions may be an important parameter for GCR simulator design due to varied responses observed for different sequences of fractionated doses [33,34]. Given estimates of average hits per cell exposed to the shielded reference field (Table 2), each human cell will be traversed by a proton ~100 times/yr, by a helium ion ~ 6 times/yr, and by an HZE ion ~0.5 times/yr. Thus, most cells in astronauts will be hit by a proton(s) before being hit by a helium or HZE ion. The ordering of the particles in the simulator has taken this into account with protons and then helium beams delivered prior to heavy ion beams to approach space-like conditions.

A second consideration in the ordering of beams was to minimize the number of unique beams (ion and energy switches) delivered to the NSRL from the Booster synchrotron. To ease operations, two low-energy protons are grouped and two low-energy helium ions are grouped sequentially throughout the delivery sequence so that only changes in the binary filter system are required. For example, a 100 MeV/n proton beam generates both the 20 MeV/n and 23 MeV/n beams with use of a degrader in the NSRL beamline. Lastly, in efforts to simulate a continuous (or highly sequential) background of protons with some helium and sporadic heavy ions, heavy ion beams are seperated by proton and helium beams. The GCR simulator supplies the beams in Table 3 in the following order *(* denotes energy in MeV/n):*

- *(H 1000*), (He 1000), (Si 600)*
- *(H 20), (H 23), (He 20), (He 23), (Ti 1000), (He 27), (He 32), (H 27), (H 32)*
- *(H 37), (H 43), (He 37), (He 43), (O 350), (He 50), (He 58), (H 50), (H 58)*
- *(H 68), (H 80), (He 68), (He 80), (C 1000), (He 100), (H 100)*
- *(H 150), (He 150), (Fe 600), (He 250), (H 250)*

This sequence requires 21 switches of unique ion-energy beams to the NSRL.

III.III.II Analysis of Dose Distribution within Animal Models

The GCR simulator is designed to expose biological targets, such as mice and rats, to the internal radiation environment seen at critical organ locations within the human body. Additionally, NASA research studies require that animal model systems are reflective of the age of astronauts which is 35 – 55 years old. Several upcoming GCR simulator studies are planning to use socially mature Wistar rats that are 5 to 9 months old and weigh approximately 700-800 grams. Given that some of the selected low energy proton and helium beams have short ranges, there is concern that these beams may stop in the animal creating a sharp dose distribution (i.e. hot spots) with the possibility of highly localized tissue responses. Additional transport studies using phantom mouse and rat models have been completed to ensure that the selected GCR simulator beam energies can provide a homogeneous dose distribution within the animal's internal organs. This explicitly now takes into account the tissue self-shielding of the rodent model system using computed tomography (CT)-based models as well as the ~2mm thickness of the exposure cages.

The Digimouse, a 3D mouse atlas from University of Southern California [http://neuroimage.usc.edu/neuro/Digimouse], is based on CT and cryosection images of a 28-g normal male mouse and has a model resolution (voxel dimension) of 0.1 mm (See Fig 7A). Each voxel has been segmented to identify major organs and tissues, including heart, liver, lungs, stomach, and brain. A larger "digirat" model is obtained here by directly scaling the Digimouse, resulting in voxel dimensions being increased by a factor of 3.15 with a resulting body mass of 754 g (Fig 7B). The voxel models have been coupled to the Monte Carlo transport code, Geant4 [35], for radiation transport of single particle beams and the complete 33 ion beam GCR simulator.

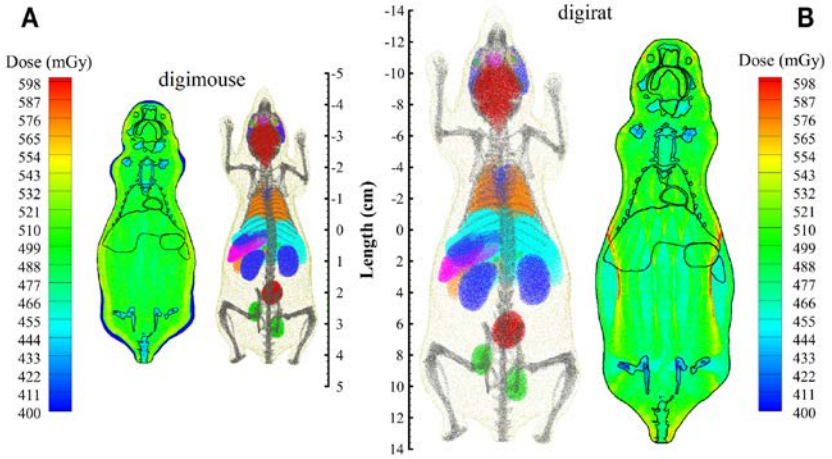

Fig 7. Digimouse has been scaled by a factor of 3.15 to obtain and estimate of a rat's body self-shielding, referred to here as "digirat." Transport of full GCR Simulation field provides homogeneous dose distribution within voxel mouse model (A) and scaled rat model (B).

The resulting dose distributions are also shown in Fig 7 for Digimouse and "digirat." Given the cage sizes and experience from "dry-runs," a pseudoisotropic irradiation (along the 6 coordinate axes) was used for the Digimouse assessment and a lateral irradiation (perpendicular to the left and right flanks) was used for the "digirat" assessment. The average dose to the Digimouse organs was 500.7 mGy comparing well to the externally delivered GCR simulator dose of 500 mGy. The dose distribution within the soft-tissues varied by less than 3%. The average voxel dose was 513.7 mGy with 95% of the voxel doses found to be within 7% of the average dose indicating no locally high dose gradients. For the "digirat," the 33 beams were oriented in a two-directional field, both laterally, on the phantom and then averaged to calculate the dose distribution. The average dose to organs was 490.7 mGy also comparing well to the externally delivered GCR simulator dose of 500 mGy. The dose distribution within the rat soft tissues varied by less than 5%. The average voxel dose was 492 mGy with 95% of the voxel doses found to be within 10% of the average also indicating a relatively smooth dose distribution. As expected with the larger animal size and beam directions limited to two orientations, a slight dose gradient is seen in both outer flanks of the "digirat" compared with the mouse. However, with the natural movement of the animal within the cage, the resulting dose gradient in the flanks will be much less than calculated above and therefore, no locally high tissues doses or hot spots are anticipated. The "digirat," weighing approximately 25 times more than Digimouse, assessment supports the expectations that body shielding from mouse cagemates will not interfere with delivering a consisitent dose distribution. Additional range considerations to deliver homogenous low-energy proton and helium dose distributions from the degraded spectra may be required for species larger than rats.

The resulting cummulative dose distributions as a function of LET are compared in Fig 8 for transport of both the full reference GCR environment and the 33 GCR simulator ion-energy beam combinations of Table 3. As shown in Fig 8, good agreement is achieved. Additional analyses are underway to consider a fluence-based approach, using both the Digimouse and voxelized rat phantom, to calculate the number of voxel traversals and cell hits within a given organ for select beams. This supports simulating the GCR environment through comparison of the number of cell hits within critical body organs of a shielded crew member and approximating the same cell hits per irradiated rodent organs in the overall beam delivery strategy.

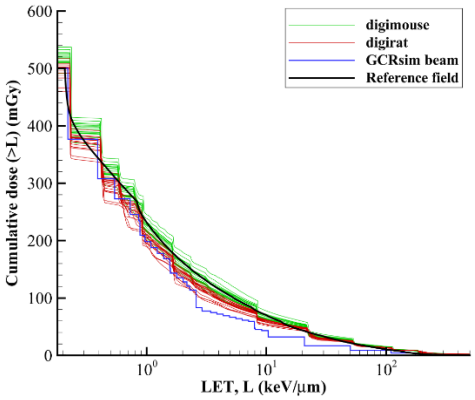

Fig 8. Cumulative dose as a function of LET comparing simulated environments within phantoms to the reference field and GCR Simulation beam exposure. Plot data available in S1 Data.

III.III.III Dose Rate Studies

Exposures from GCR consist of a complex field of many different types of particles that deposit dose at a relatively low rate. Data on dose-rate effects for higher LET radiation and more specifically dose-rate effects in a space-like environment are limited. Evidence suggests that biological responses seen at high dose rates may be different than those that occur at the lower rates seen in space [2]. Animal experiments using multiple small dose fractions and/or very low-dose rates of densely-ionizing radiation are needed to reduce uncertainties in predicting risk at space-relevant dose rates [36,37]. Likewise, evaluation of countermeasure efficacy may also depend on dose rate.

Thus, a significant challenge for space radiobiology research is developing strategies to simulate a chronic GCR exposure of up to 3 years, approximating a Mars mission, in relation to simulations with animal models of human

risks. To more closely simulate the low dose rates found in space, single ion and mixed field exposures can be divided into a large number of fractions over long periods of time (e.g., daily fractions over two to six weeks). Individual beam fractions as low as 0.1-0.2 mGy can be reliably measured and delivered at the NSRL (See NSRL Facility Modifications Section). The goal is to design a highly fractionated simulation scheme, within animal and facility operational constraints, such that the time scale of a biological response becomes primarily a function of dose (i.e., insensitive to dose rate) to more closely mimic the space environment. Computational analyses of accelerator GCR simulations have shown that a large percentage of cells will be hit with two or more particles in simulated chronic exposures of a week or less, and recommend exposures of several weeks with times approaching 30 days or longer to avoid any high dose-rate artifacts [38,39]. Likewise, considering the relative life span of humans compared with mice, in which 32 human days are estimated to roughly scale to 1 mouse day [40], a duration of approximately 30 mouse days is suggested to mimic a 3-year human exploration mission duration. Thus, the first chronic GCR simulator studies will attempt to scale to both dose rate and life span.

NASA baseline chronic GCR simulations will expose animal models to highly fractionated doses for 6 days/week over a two to four week period. The seventh day of the week is reserved for contingency in case of unforeseen operational difficulties. Total exposures are 250 mGy (over 2 weeks; delivered in 12 fractions), 500 mGy (over 4 weeks; delivered in 24 fractions) and 750 mGy (over 6 weeks; delivered in 36 fractions). The total daily dose of 20.8 mGy and dose fraction from each ion group is fixed allowing for 3 dose points delivered on the same fractionation schedule. As an example, for a four-week chronic 500 mGy exposure each of the 33 beams (shown in Table 3) will be delivered daily in 24 equal fractions with proton doses delivered daily in 0.3 to 5.1 mGy fractions, He doses delivered in 0.1 to 1.0 mGy fractions, and HZE particle doses delivered in 0.17 to 0.49 mGy fractions. These fractionated schemes rely on the ability to repeatedly deliver small doses and impose additional constraints limiting the number of HZE particles selected to represent the design reference field. Given facility, operational and animal considerations, continuous exposures are not feasible. While highly fractionated doses can begin to more closely mimic the space environment, giving daily fractions provides time for radiation induced damage repair which may not occur in deep space. On-going cellular research studies at NSRL are investigating these effects to provide additional evidence for future simulations. Similarly, low dose rate, high LET studies are being performed with neutrons to continuously irradiate rodents which collectively will be used to inform risk estimates.

Other parameters exist to approach a low dose-rate limit or a region of operations such that particle hits are independent on relevant biological timescales. Under these conditions, results should be scalable to the very low dose and dose rates of the space environment. Witihin the current implementation strategy, three parameters are adjustable: the dose fraction (mGy) of ions delivered, the dose rate of delivery (cGy/min), and the time between daily particle doses (from minutes to hours to days). Facility operations constrain the flexibility of solutions given: low dose fractions must be reliably and repeatedly delivered and measured by NSRL dosimetry, the dose rate is limited by the spills per cycle as dictated by the operation of the Department of Energy's Relativistic Heavy Ion Collider (RHIC) at BNL, and the time between the 33 daily particle doses is limited by the duration animals can be housed in the target room (typically 8 to 10 hours). Other schemes to approach a low dose-rate limit include the delivery of the GCR simulator on a different daily schedule, for example three times a week over a longer time course.

To improve our understanding of dose and dose-rate effects (DDREF) [41], NASA guidance requires that chronic studies include an acute exposure at an equivalent dose. Given the continuous low-dose rates found in space (< 1 mGy/day), challenges remain in simulating the galactic cosmic ray environment in Earth-based analogs [7]. Modeling is expected to play a key role in interpreting and translating biological results from acute (high dose rate) and fractionated exposures to the protracted [37] and mixed-field [42] exposures humans see in space.

III.III.IV Simplified 5-Ion GCR Simulator

NASA has also defined a "Simplified 5-ion GCR Simulator" beam for use in the initial understanding of sequential-field quality effects, collection of preliminary data to power studies, as well as for use in countermeasure screening studies. The ion-energy beam combinations are defined in Table 4 and require less time to deliver compared with the full 33-ion GCR simulation. The order of beam delivery and dose fractions are consistent with the full GCR simulator (Table 3), with proton irradiation first and last in the sequence as well as delivering the majority of exposure. Although aspects of the spectral characteristics of the reference field are lost in not capturing the full LET dependence

of the low energy protons and helium components, the selected beams will provide uniform dose profiles within both mice and rats given that the ion ranges greatly exceed animal tissue thicknesses. This is also the case with larger rats given that they remain flank to the incoming beam (i.e., not nose-to-tail).

Table 4. Simplified 5-ion mixed field normalized to 500 mGy.

Ion species	Energy (MeV/n)	LET (keV/ µm)	Range (cm)	Dose (mGy)	Percent contribution to total dose (%)	delivery order	Fractionated dose- 24 exposures (mGy/day)
^{1}H	1000	0.2	326.6	174.1	35	1	7.3
^{28}Si	600	50.4	22.7	5.7	1	2	0.2
^{4}He	250	1.6	38.3	90.2	18	3	3.8
^{16}O	350	20.9	16.9	29.1	6	4	1.2
^{56}Fe	600	173.8	13.1	5.1	1	5	0.2
^{1}H	250	0.4	38.1	195.9	39	6	8.2
			total	*500.0*			*20.8*

While the full NSRL GCR simulator is being used to deepen our understanding of well-characterized model systems and to test hypotheses related to mixed field and chronic (highly fractionated) exposures, studies of relatively less mature model systems that lack deep historical data sets of single ions are generating research results using the simplified field. Results from the simplified field support the development of predictive models where our understanding of ion dependency/inter-dependency is limited, especially with respect to potential central nervous system decrements. The shorter time for acute and chronic irradiations can increase NSRL throughput of animals, especially in the case of rat studies, where each cave entry to the target room is limited to 15 animals for the large beam configuration. Likewise, constraints on cell culture systems may also benefit from the shorter irradiation times. Updates to the Simplified 5-ion GCR simulator will be based on experimental consortium results, mixed field studies, and model predictiions as well as results from the full 33-beam GCR simulator.

IV. RESULTS

Operating the GCR simulator requires the ability to rapidly and reliably change between multiple ion-energy beam combinations and repeatedly deliver them to an experimental target at predetermined doses. Facility modifications, including both hardware and software efforts, supporting full GCR operations at the NSRL, were completed in early 2017. The system was commissioned at Brookhaven National Laboratory in late 2017 and first used in 2018 for major PI-led research studies.

IV.I. NSRL Facility Modifications

Investments in advanced ion source technology and control systems were essential to enable a mixed-field irradiation capability. GCR simulator ion beams are extracted from BNL's Booster synchrotron and transported to the shielded target room within the NSRL facility as shown in Fig 9. Three sources can supply ions to the Booster including the LINAC (protons only), the Tandem Van de Graaff (ions and protons), and the Electron Beam Ion Source (EBIS) (any ion except protons) [43]. The GCR simulator relies on EBIS for helium and heavy ions and either the LINAC (Linear Accelerator) or Tandem for protons. EBIS has two ports for gas sources that are manually changed to switch between ion species generated. Helium occupies one of those ports during GCR simulations. In late 2013, EBIS was equipped with a Laser Ion Source (LIS) which has the capability to produce ions from many different solid targets as well as to rapidly switch between solid-source targets through automated controls software. Modifications to fit the LIS's vacuum chamber with a translation table enabled the installation of the specific solid targets needed for the production of ^{12}C, ^{16}O, ^{28}Si, ^{48}Ti, and ^{56}Fe required by the simulator. With these control modifications and helium gas provided as a source, ion and energy changes are achieved by a single command in less than two minutes [43]. In late 2016, a variable thickness stripping foil changer was installed at the upstream end of the D6 septum magnet to

improve control of source-beam optics after Booster extraction and prior to injection into the NSRL beam line. The foil changer consists of 8 individual thicknesses of foils from 0.25 to 16 mil (6.35×10^{-4} cm to 4.064×10^{-2} cm) with the thinnest foils made of aluminum and the thicker foils ($\geq$1mil or $\geq 2.54 \times 10^{-3}$ cm) made of copper which are remotely controlled in the beam line to provide a range of thicknesses from 0.25 to 63.75 mils (6.35×10^{-4} to 1.619×10^{-1} cm). This upgrade from the previous two foil filter system enables better control of the beam shape at the target location in switching from one ion-energy combination to another [43].

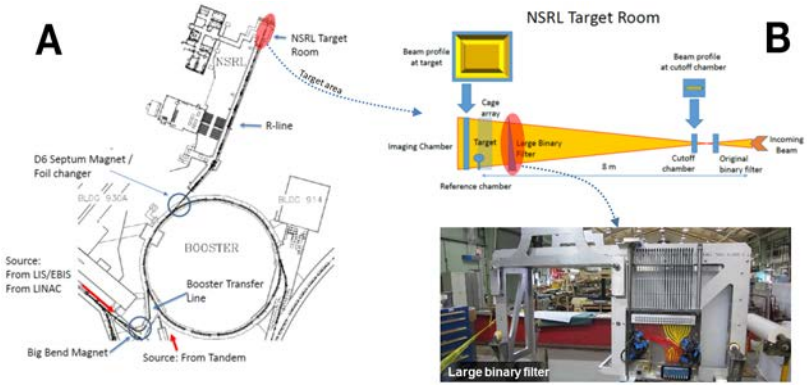

Fig 9. Facility layout of NSRL at BNL. (A) Tools to reliably control system hardware settings, from ion production by the LIS through booster injection, acceleration, extraction and delivery to the NSRL target room were developed to sequentially deliver the GCR simulator ion-energy beam combinations. (B) Position of imaging chamber behind target (top, left hand side), cut-off chamber (top, right hand side) near beam entrance to target room, and photo of large area degrader (binary filter) system (bottom) in NSRL beam line to maintain control and uniformity of 60 by 60 cm^2 beam.

The software controlling the order and dose of ion-energy beam combinations to the target is run locally from the NSRL dosimetry console. After ion production at the source, all hardware control settings along the beam lines including moving species through the EBIS, the transfer line to the Booster (including the big-bend magnet), the Booster itself (injection and extraction), and the NSRL beam line (R-line) must be able to change to sequentially deliver different beams within a reasonable amount of time (Fig 9). A single software application was developed and extensively tested to reliably move from one hardware setting to another. The simulator control file contains the sequential list of ion-energy-dose combinations (Table 3) to which various elements of the accelerator and dosimetry systems must respond in a precisely choreographed sequence. The ion-energy beam combinations are selected and controlled by the BNL complex-wide Linux cluster while a NSRL local software program controls dose delivered using essentially a dose-based beam cut-off system. Incremental demonstration of the modified system was successfully demonstrated in 2016 with the delivery of H, Si, and Fe ions to the NSRL target room in a single day. Chronic GCR simulations require the delivery of individual beam fractions as low as 0.1-0.2 mGy which represented a significant operational challenge for dosimetry and imaging systems (Fig 9B top). With the simulator running since late 2018, NSRL has demonstrated the capability to image the beam at such low dose rates, to retain sufficient monitoring and control over the beam shape, and to reliably measure the low daily doses specified for each beam.

The GCR simulator can be delivered in a 20 x 20 cm^2 or in a larger 60 x 60 cm^2 beam configuration. Typical dose rates of ~10 Gy/min and ~0.5 Gy/min are available for the 20 x 20 cm^2 and the 60 x 60 cm^2 configurations, respectively. Beam uniformity is monitored with segmented thin ion chambers and fluorescent screen techniques during beam preparation and dose delivery. The ion chamber is capable of measuring differences in intensity of 2-3% over the 60 x 60 cm^2 area. A large-area degrader system was installed approximately 1 m upstream of the target location to enhance spatial uniformity across the 60 x 60 cm^2 beam spot (See Fig 9B) which allows for the full utilization of the beam area. The binary filter thicknesses are the same thicknesses as the previous system ranging from 0.1, 0.2, …. 12.8 cm of polyethlylene (with a density of 0.93 g/cm^3). The resolution of this system enables verification of incoming beam energies through Bragg curve/range measurements which is especially important for the lowest energy proton and helium beams utilized in the simulation. Due to its close proximity to the target, these energy-degraded beams do not lose their shape and maintain good uniformity in dose, intensity, and calibration quality.

Each GCR simulation run requires 21 switches of unique ion-energy beam combinations to the target room. Switch times range between ~2 to 4 minutes with longer switch times required for He species to wait for the EBIS to clear prior to the introduction of a new species. The additional 12 beams (lower energy H and He) are generated via the binary filter in the NSRL beam line. Approximately 70 to 75 minutes is required to deliver the doses from all 33 beams for either acute (250 to 750 mGy) or daily fractionated exposures which may pose a challenge for certain animal or cell model systems. The simplified 5-ion GCR simulation requires approximately 20 to 25 minutes to deliver either acute or fractionated exposures. Additional software records dose over each individual GCR simulation ion as well as cumulative dose for both acute and fractionated dose-rate protocols. Each investigator is provided with a detailed record of the absorbed dose in tissue and the duration of each radiation exposure. Fig 10 shows dose tracking of the individually delivered ions as viewed on the NSRL dosimetry console.

Fig 10. Computer screen shot measuring GCR simulator doses per ion for the 20.8 mGy cycle. On average, the cycle took ~70 to 75 minutes of which over 50 minutes were devoted to beam switching.

IV.II Animal and Cell Handling

In the large beam spot (60 x 60 cm^2), 54 special housing cages, configured in a 9 by 6 array, can accommodate at least 2 and sometimes 3 mice each (depending on size) for the 70 - 75 minute irradiation period (Fig 11A). The resulting range of subjects per exposure is 108-162 (with the high end of this range being very ambitious). The large beam can accommodate 15 special rat housing cages configured in a 3 by 5 array capable of holding 1-2 rats each depending on size and orientation (Fig 11B). Special vents are provided in the tops of the cages with air circulation provided by external fans (Fig 11C). Blowing air across the loaded array while animals are waiting to be transported to the target room as well as during the irradiation period is essential. An isopad is added in the bottom of the cage. For cell experiments, a large incubator has been modified for use in the 60 x 60 cm^2 sized beam as shown in Fig 12A. Holders for both T75 and T25 flasks are available to experimenters (Fig 12B).

Fig 11. Housing array for mouse (panel A) and rat (panel B) irradiations in the 60 x 60 cm^2 beam. Exposure boxes, made of ~2mm thick polyethylene, stack together and are held in an array using a fabricated frame strucure. (C)

Ventilation lids for air circulation are provided. The nonventilated sides of the lids are painted red to serve as a quick visual cue that the lids are in the correct orientation for air flow.

Fig 12. Modified incubator for use in beamline (A) with a holder that can accommodate up to fifteen T75 flasks in a 3 by 5 array or forty four T25 flasks (B).

The cages for mouse exposures have interior dimensions of 10 x 10 x 4.5 cm in size providing plenty of space for movement. For acute irradiations, NASA guidance has limited the number of animals to 2 mice per cage or 1 rat per cage to avoid any ion range (Bragg peak) issues associated with body shielding from cagemates. For fractionated irradiations, the maximum cage capacity is limited to three mice and possibly two smaller rats. In this case, the positioning of the animals will be random during each daily fraction. Specialized rat cages have interior dimensions of 19.5 x 10.5 x 9.5 cm and also permit a significant amount of movement during exposures, even for the larger male Wistar rats weighing on the order of 700-800 g. The 19.5 cm length of the box is perpendicular to the beam to provide a lateral or flank exposure. Larger rats are unable to position themselves 'nose-to-tail' in the beam direction. Based on a 90 minute dry run, with two Wistar rats, one rat turned 44 times in 90 minutes whereas the second rat turned 130 times in 90 minutes, thus exposing both flanks to the incoming beam direction. This active randomized movement helps provide homogenous dose distributions within larger animals during irradiations (See Analysis of Dose Distribution within Animal Models Section).

V. DISCUSSION

Past ion source and control technology at accelerator facilities limited decades of biological research to studying model systems acutely exposed to a single ion. These studies are expensive and require large cohorts of animals and/or time consuming cellular assays to obtain each ion-specific data set. Given the complexity of the space radiation environment, numerous studies spanning relevant ions and energies across multiple model systems and endpoints are required to quantify and mitigate radiogenic health risks faced by astronauts. Major scientific questions on the additivity of biological responses from single ion data and the effect of dose rate remain:

- *Is there synergy, antagonism, or neither in space radiation-induced tumorigenesis, cardiovascular disease, or CNS decrements after mixed GCR-like exposures compared to that predicted from results with individual ion beams?*
- *How should dose-rate modifiers be implemented in models of risk to scale from acutely exposed human terrestrial cohorts (low LET gamma) to astronauts who are chronically exposed to a mixed field of low- and high-LET ions?*
- *Will dose-rate scale risk inversely, conventionally, or have no effect?*
- *Can a ground-based analog operate in a low dose and dose rate regime that sufficiently mimics the space environment to validate countermeasures?*

Answers to these questions were previously inaccessible utilizing ground-based irradiation facilities. Space-based research platforms beyond low-Earth orbit and outside Earth's protective magnetosphere do not exist. Although flight studies are recognized as an important component in characterizing and mitigating radiogenic health risks, the scientific evidence is largely expected to be acquired on the ground. Until now, there were no ground-based facilities in the world capable of simulating the mixed-field GCR environment.

Major NASA deliverables supporting human exploration include models to quantify risk, development of permissible exposure limits, and countermeasures to mitigate health risks. With decades of single ion research spanning particle types and LET, NASA's cancer risk model and cancer permissible exposure limits (PEL's) are most mature [31,44]. However, important questions remain on the validity of simple additivity and use of dose rate modifiers in estimating risk from chronic mixed-field exposures which better simulate the space environment. The development of risk models and validating PELs, in the units of Gy-Eq, for the risks of cardiovascular disease (CVD) and potential central nervous system decrements are less mature with radiation quality effects largely unknown [44,45]. GCR simulation research studies have the ability to accelerate early CVD and CNS PEL development using a mixed-field quality factor (QF) and dose-rate (DREF) modifier assessed in single studies rather than through a multitude of acute ion by ion exposures with the need to then assess and validate additivity and dose rate modification. An equally important goal of the GCR simulator is to provide a space relevant environment to accelerate biological countermeasure testing for risk mitigation. Countermeasure evaluation across multiple radiogenic risks, drug dosages, and ion types supposes a large test matrix of conditions which can quickly become cost prohibitive. NASA's approach to targeting countermeasures with the ability to reduce multiple risks through reduction of common indicators, for example inflammation, and testing efficacy in the highly-fractionated, mixed-field environment of the GCR simulator can significantly reduce costs and accelerate identification and validation efforts. Although it is recognized that single ion studies are still important in quantifying risk dependence on LET (or Z and E) to gain mechanistic insight on the interaction of radiation at the cellular and tissue level and its dependence on radiation quality. This information may be especially important in generating hypotheses to inform countermeasure development. Although the GCR Simulator does not represent the detailed LET spectra for all shield designs and time in solar cycle, differences in the internal spacecraft environment spectrum compared with the ability to simulate in a ground based facility with discrete monoenergetic ion beams is deemed small in comparison [11].

The GCR simulator reference environment and implementation strategy were baselined in 2017. As experimental results become available, updates to field parameters can be easily incorporated including increasing the number of discrete ion and energy beams used or modifying existing ion-energy beam combinations. Given the success of operations to date, potential updates can confidently include ~10-12 species of particles with $Z \geq 3$ generated by the LIS. However as the number of ions are increased, the dose delivered from each ion decreases and will be limited by the ability of the current NSRL dosimetry systems to reliably deliver and measure small doses, especially when moving to highly-fractionated delivery schemes. With current operational capabilities, 0.1 to 0.2 mGy is the limiting low dose. However, other strategies to increase the number of representative HZE particles to generate a more continuous high LET distribution may include moving to a different fractionation scheme where protons and helium are delivered daily while distinct HZE particles are delivered on a different schedule. Given that the secondary environment experienced by crew (within a shielded vehicle) is largely comprised of protons and helium with a rare HZE interaction (Table 2), other schemes to provide H and He for several cycles prior to a heavy ion may be a more realistic representation of the reference environment and alleviate low dose constraints.

Other concepts have explored the use of absorbers in the beamline to attenuate and fragment heavy ions as a means to spread both the energy and fragment distribution to approximate the GCR environment found within spacecraft. Kim and colleagues, 2015 [38] suggests the use of simple slabs of polyethylene with 9 heavy-ion beams in addition to protons and helium; whereas Chancellor and colleagues, 2018 [46], suggest the use of a more sophisticated absorber in geometry and material selection with a single incident ion to simulate the complex mixture of nuclei and energies, including the secondary production of neutrons. As discussed, hybrid approaches are under consideration by NASA which include the possibility of adding higher-energy incoming beams incident on specially designed absorbers/moderators in the beam line (Fig 3).

Research is progressing to quantify mixed field radiation quality effects, dose, and dose rate effects in multiple cellular and animal model systems. Modelling approaches are being developed to leverage historical data sets of acute single ion experiments to determine simple additivity, synergistic, or antagonistic effects on risk characterization in a mixed field as well as to quantify the impact of acute versus chronic exposures on existing data sets. Key simulation challenges remain in determining whether the delivered field of mixed ion species adequately approximates the GCR environment for radiobiology endpoints of interest, in understanding how best to implement dose-rate studies to better simulate chronic deep-space exposures, and in the selection of appropriate animal and cell models supporting translation to humans. Results from early experiments are forthcoming and will inform future modifications to reference field specifications and implementation strategy for improved ground-based GCR simulations at the NSRL.

Abbreviations:

BFO, blood forming organ; BNL, Brookhaven National Laboratory; CNS, central nervous system; CVD, cardiovascular disease; DDREF, dose and dose-rate effectiveness factor; DOE, US Department of Energy; EBIS, Electron Beam Ion Source; EM, electromagnetic; GCR, galactic cosmic radiation; HZE, high charge and high energy ions; LEO, low Earth orbit; LET, linear energy transfer; LIS, laser ion source; MSLRAD, Mars Science Laboratory radiation assessment detector; n, nucleon; NCRP, National Council on Radiation Protection; NSRL, NASA Space Radiation Laboratory; OLTARIS, On-Line Tool for the Assessment of Radiation in Space; π/EM, pions and electromagnetic radiation; Q, quality factor; RBE, relative biological effectiveness; REID, risk of exposure induced death; SPE, solar particle event.

REFERENCES

1. NASA. Artemis Plan: NASA's Lunar Exploration Program Overview. National Aeronautics and Space Administration, Washington DC, Sept. 21, 2020. [https://www.nasa.gov/sites/default/files/atoms/files/artemis_plan-20200921.pdf] (Accessed October 1, 2020).
2. National Council on Radiation Protection (NCRP). Information needed to make radiation protection recommendations for space missions beyond low-Earth orbit. NCRP Report 153, Bethesda, Maryland; 2006.
3. National Research Council (NRC). Health risks from exposure to low levels of ionizing radiation. BEIR VII Phase 2 report. National Academies Press; 2006.
4. Durante M, Cucinotta FA. Physical basis of radiation protection in space travel. Rev. Mod. Phys. 83, 2011. pp. 1245-1281.
5. Introduction to track structure and z*2/β2. Curtis SB. https://three.jsc.nasa.gov/articles/Track-Structure-SCurtis.pdf. Date Posted: 02-29-2016
6. Schimmerling W. Genesis of the NASA Space Radiation Laboratory Life Sci Space Res. 2016. Epub 2016 Mar **7.**
7. Norbury JW, Schimmerling W, Slaba TC, Azzam EI, Badavi FF, Baiocco G, and colleagues, Galactic cosmic ray simulation at the NASA Space Radiation Laboratory. Life Sciences in Space Research, 8, 2016. pp 38-51.
8. Sihver L. Physics and biophysics experiments needed for improved risk assessment in space. Acta Astronautica 63, 2008. pp. 886-898.
9. Slaba TC, Blattnig SR, 2014. GCR environmental models I: Sensitivity analysis for GCR environments. Space Weather 12, 2014. pp. 217-224.
10. Townsend LW, Nealy JE, Wilson JW, Simonsen LC. Estimates of galactic cosmic ray shielding requirements during solar minimum. NASA TM-4167, 1990.
11. Slaba TC, Blattnig SR, Norbury JW, Rusek A, La Tessa C. Reference field specification and preliminary beam selection strategy for accelerator-based GCR simulation. Life Sciences in Space Research, 8, 2016. pp. 52-67.
12. Norbury JW, Slaba TC. Space radiation accelerator experiments – The role of neutrons and light ions. Life Sciences in Space Research, 3, 2014. pp. 90-94.
13. Walker SA, Townsend LW, Norbury JW. Heavy ion contributions to organ dose equivalent for the 1977 galactic cosmic ray spectrum. Adv. Space Res. 51, 2013. pp. 1792-1799.
14. Slaba TC, Qualls GD, Clowdsley MS, Blattnig SR, Walker SA, Simonsen LC. Utilization of CAM, CAF, MAX, and FAX for space radiation analyses using HZETRN. Advances in Space Research 45, 2010. pp. 866-883.
15. O'Neill PM. Badhwar-O'Neill galactic cosmic ray flux model – revised. IEEE Trans. Nuc. Sci., **57**: 2010. pp. 3148–3153.
16. Wilson JW, Townsend LW, Schimmerling WS, Khandelwal GS, Khan F, Nealy JE, and colleagues, Transport methods and interactions for space radiations. NASA RP-1257, 1991.
17. Slaba TC, Blattnig SR, Badavi FF. Faster and more accurate transport procedures for HZETRN. J. Comp. Phys. 229, 2010. pp. 9397-9417.
18. Slaba TC, Blattnig SR, Aghara SK, Townsend LW, Handler T, Gabriel TA, and colleagues, Coupled neutron transport for HZETRN. Radiat. Meas. 45, 2010, pp. 173-182.

19. Kramer R, Vieira JW, Khoury HJ, Lima FRA, Fuelle D. All about MAX: A Male Adult Voxel Phantom for Monte Carlo Calculations in Radiation Protection Dosimetry. Physics in Medicine and Biology, Volume 48, 2003. pp. 1239-1262.
20. Kramer R, Vieira JW, Khoury HJ, Lima FRA, Loureiro ECM, Lima VJM, Hoff G. All about FAX: A Female Adult Voxel Phantom for Monte Carlo Calculations in Radiation Protection Dosimetry. Physics in Medicine and Biology, Volume 49, 2004. pp. 5203-5216.
21. Simonsen LC, Nealy JE. Radiation protection for human missions to the moon and Mars. NASA Technical Paper 3079, 1991.
22. Slaba TC, Mertens CJ, Blattnig SR. Radiation shielding optimization on Mars. NASA Technical Paper-217983, 2013.
23. Cucinotta FA, Kim MY, Ren L. Managing lunar and Mars mission radiation risks Part I: Cancer risks, uncertainties, and shielding effectiveness. NASA Technical Paper-213164, 2005.
24. Norbury JW, Slaba TC, Aghara S, Badavi FF, Blattnig SR, Clowdsley MS, and colleagues, "Advances in space radiation physics and transport at NASA." Life Sci Space Res (Amst) 22, 2019. pp 98-124.
25. Matthia D, Hassler DM, de Wet W, Ehresmann B, Firan A, Flores-McLaughlin J, and colleagues, The Radiation Environment on the Surface of Mars – Summary of model calculations and comparison to RAD data. Life Sciences in Space Research, Volume 14, 2017. pp. 18-28.
26. Slaba TC, Blattnig SR, Reddell B, Bahadori A, Norman RB, Badavi FF. Pion and Electromagnetic Contribution to Dose: Comparisons of HZETRN to Monte Carlo Results and ISS Data. Advances in Space Research, Volume 52, 2013. pp. 62-78.
27. Slaba TC, Blattnig SR, Clowdsley MS. Variation in Lunar Neutron Dose Estimates Radiation Research **176**, 2011. pp. 827–841. DOI: 10.1667/RR2616.1
28. Matthia D, Hassler DM, de Wet W, Ehresmann B, Firan A, Flores-McLaughlin J, Guo, J, Heilbronn LH, Lee K, Ratliff H, Rios RR, Slaba TC, Smith M, Stoffle NN, Townsend LW, Berger T, Reitz G, Wimmer-Schweingruber RF, Zeitlin C. The Radiation Environment on the Surface of Mars – Summary of model calculations and comparison to RAD data. Life Sciences in Space Research, **14**, 2017. pp. 18-28.
29. Zeitlin C, Hassler DM, Cucinotta FA, Ehresmann B, Wimmer-Schweingruber RF, Brinza DE. and colleagues, Measurements of energetic particle radiation in transit to Mars on the Mars Science Laboratory. Science 340, 2013. pp. 1080-1084.
30. National Council on Radiation Protection and Measurements. Recommendations of Dose Limits for Low Earth Orbit. NCRP Report 132, Bethesda MD; 2000.
31. Cucinotta FA, Kim MY, Chappell LJ. Space radiation cancer risk projections and uncertainties – 2012. NASA TP 2013-207375, 2013
32. International Commission on Radiological Protection (ICRP). Recommendations of the International Commission on Radiological Protection. ICRP Publication 60. Pergamon Press; 1991.
33. Sasi SP, Yan X, Zuriaga-Herrero M, Gee H, Lee J, Mehrzad R, and colleagues, Different Sequences of Fractionated Low-Dose Proton and Single Iron-Radiation-Induced Divergent Biological Responses in the Heart. Radiation Research 188(2), 2017. pp. 191-203. doi: 10.1667/RR14667.1. Epub 2017 Jun 14.
34. Zhou G, Bennett PV, Cutter NC, Sutherland BM. Proton-HZE-Particle sequential dual-beam exposures increase anchorage-independent growth frequencies in primary human fibroblasts. Radiation Research 166 (3), 2006, pp. 488-494. https://doi.org/10.1667/RR0596.1
35. Agostinellie, S, Allison J, Amako K, Apostolakis J, Araujo H, Arce P. Geant4 – a simulation toolkit. *Nucl. Instr. Meth. A* 506, 2003. pp. 250-303.
36. National Council on Radiation Protection (NCRP). Radiation Protection for Space Activities: Supplement to previous recommendations. *NCRP Commentary 23.* Bethesda, Maryland; 2014.
37. Shuryak I, Brenner DJ. Mechanistic modeling predicts no significant dose rate effect on heavy-ion carcinogenesis at dose rates relevant for space exploration. Radiation Protection Dosimetry, 183(1-2), 2019. pp. 203-21. doi:10.1093/rpd/ncy223.
38. Kim MY, Rusek A, Cucinotta FA. Issues for simulation of galactic cosmic ray exposures for radiobiological research at ground-based accelerators. Front. Oncol. 5:122, 2015. doi: 10.3389/fonc.2015.00122
39. Cucinotta FA, Alp M, Sulzman FM, Wang M. Space radiation risks to the central nervous system. Life Sciences in Space Research 2, 2014. pp. 54–69. http://dx.doi.org/10.1016/j.lssr.2014.06.003
40. National Council on Radiation Protection (NCRP). Extrapolation of radiation-induced cancer risks from non-human experimental systems to humans. NCRP Report No. 150. Bethesda, Maryland; 2005.
41. A Note On The Dose-Rate-Effectiveness Factor and its Progeny DDREF. Fry RJM. https://three.jsc.nasa.gov/articles/DDREF.pdf. Date posted: 01-07-2013.

42. Huang EG, Wang RY, Xie L, Chang P, Yao G, Zhang B, and colleagues, Simulating galactic cosmic ray effects: synergy modeling of murine tumor prevalence after exposure to two one-ion beams in rapid sequence, Life Sciences in Space Research, 2020. https://doi.org/10.1016/j.lssr.2020.01.001
43. La Tessa C, Sivertz M, Chiang IH, Lowenstein D, Rusek A. Overview of the NASA Space Radiation Laboratory. Life Sci Space Res (Amst), 11, 2016, pp. 18-23. https://doi.org/10.1016/j.lssr.2016.10.002
44. NASA Space Flight Human System Standard. NASA STD 3001, Vol I; 2014.
45. National Council on Radiation Protection and Measurements. Radiation Exposure in Space and the Potential for Central Nervous System Effects: Phase II. NCRP Report 183, Bethesda MD; 2019.
46. Chancellor JC, Blue RS, Cengel KA, Auñón-Chancellor SM, Kathleen H, Rubins KH, *and colleagues.* Limitations in predicting the space radiation health risk for exploration astronauts. *npj Microgravity* 4, 8, 2018. doi:10.1038/s41526-018-0043-2